Stability diagrams of plasma-embedded three-unit-charge systems: Borromean states and the Efimov effect

Federico Pont* and Pablo Serra†
Facultad de Matemática, Astronomía y Física, Universidad Nacional de Córdoba and IFFAMAF (CONICET), Ciudad Universitaria, 5000 Córdoba, Argentina
(Received 30 December 2008; published 16 March 2009)

The stability of the ground state of three-unit charge $q_i=\pm 1,\pm 1\mp 1$, interacting through a statically screened Coulomb potential, has been studied as a function of the values of the constituent masses for different values of the screening parameter. General conditions are given and accurate variational calculations have been performed to determine the region where the three-body ground state is Borromean. The possible existence of Efimov states when the screening parameter is equal to the two-body critical screening parameter is discussed. The critical exponent for the energy in different regions of the stability diagram has been also calculated.

DOI: 10.1103/PhysRevA.79.032508 PACS number(s): 31.15.ac, 31.15.xt, 36.10.−k

I. INTRODUCTION

The study of the stability of bound states near the continuum threshold has attracted much interest since the pioneering work of Bethe [1] and Hylleraas [2] confirming the existence of the H^- anion. Recently, the stability of other three-body Coulomb systems was studied and it is known that the stability of these systems depends crucially on the mass of the constituents [3–5]. It was shown that, for systems made of three unitary charges $\pm(1,1,-1)$, there are stable structures such as (p,p,e^-) and (e^+,e^+,e^-) while other systems are unbound such as (p,e^+,e^-).

New phenomena appear when these kinds of systems are embedded in a Debye plasma and the Coulomb interactions are screened. A simple form to describe such screening is to replace the long-range Coulomb interaction by the short-range Yukawa potential $\exp(-\sigma r)/r$. The screening parameter σ simulates different plasma conditions, from $\sigma=0$, which corresponds to vacuum, to large values of σ describing thermal ionization in plasma.

Previously reported three-body systems in plasma included H_2^+, $pp\mu^-$, Ps^-, and H^- [6–9]. In the case of H_2^+ it was found that the ground state is Borromean [6]. An N-body bound state is called Borromean if all possible subsystems are unbound. For $N=3$ it means that the H^--like atom or the H_2^+-like molecule is bound but the corresponding H-like atom is unbound. Most examples are found in nuclear physics as a consequence that Borromean states present halos [10], although not every halo nuclei has a Borromean nature. Another feature of some three-body systems is the existence of Efimov effect [11]. The Efimov effect is a direct consequence of the different ranges of the interacting potentials [12,13] and it emerges from the resonant coupling of two-body interactions. Both phenomena are closely related because Borromean states also arise in the Efimov effect. We are going to see that the Borromean state of H_2^+ could actually be an Efimov trimer. Other example of Borromean binding in atomic and molecular physics is the case of the ^{3}He atom. The $(^3\mathrm{He})_2$ molecule is unbound, but it is known that liquid helium is stable, so there must be a number N such that $(^3\mathrm{He})_N$ is bound. The last known upper bound for this number is $N=35$ obtained by Guardiola and Navarro [14].

The fact that the screened H_2^+ is Borromean motivated us to search an extension of the stability domain where the ground state is Borromean and look for possible existence of Efimov states. In this work we present the stability diagram of the ground state for a system of three-unit charges $\pm(1,1,-1)$ interacting through the Yukawa potential as a function of the three masses and the screening parameter σ. In Sec. II the model is described. The numerical calculations were done applying a variational method explained in Sec. III. In Sec. IV the stability diagrams in the inverse masses barycentric coordinates are shown for several values of the screening σ. The possible existence of Efimov states is discussed in Sec. V. In Sec. VI the critical exponent for the energy is calculated, and finally, in Sec. VII our conclusions are presented.

II. THREE-BODY HAMILTONIAN

The Hamiltonian for three unitary charges $q_1=q_2=\pm 1$; $q_3=\mp 1$ interacting through Yukawa potentials, in atomic units, is

$$\mathcal{H}=-\frac{1}{2m_1}\nabla_1^2-\frac{1}{2m_2}\nabla_2^2-\frac{1}{2m_3}\nabla_3^2+\frac{e^{-\sigma|\vec{r}_1-\vec{r}_2|}}{|\vec{r}_1-\vec{r}_2|}-\frac{e^{-\sigma|\vec{r}_2-\vec{r}_3|}}{|\vec{r}_2-\vec{r}_3|}-\frac{e^{-\sigma|\vec{r}_1-\vec{r}_3|}}{|\vec{r}_1-\vec{r}_3|}. \quad (1)$$

After the usual center-of-mass reduction

$$\left.\begin{matrix}\vec{r}_1\\ \vec{r}_2\\ \vec{r}_3\end{matrix}\right\}\rightarrow\left\{\begin{matrix}\vec{R}_{\mathrm{CM}}\\ \vec{r}_1-\vec{r}_3\\ \vec{r}_2-\vec{r}_3\end{matrix}\right.$$

and omitting the term corresponding to the center-of-mass kinetic energy, the Hamiltonian takes the form

*pont@famaf.unc.edu.ar
†serra@famaf.unc.edu.ar

$$\mathcal{H} = -\frac{1}{2\mu_1}\nabla_1^2 - \frac{1}{2\mu_2}\nabla_2^2 - \frac{1}{m_3}\nabla_1\nabla_2 - \frac{e^{-\sigma r_1}}{r_1} - \frac{e^{-\sigma r_2}}{r_2} + \frac{e^{-\sigma r_{12}}}{r_{12}}, \tag{2}$$

where $r_{12}=|\vec{r}_1-\vec{r}_2|$ and $\mu_i=\frac{m_i m_3}{m_i+m_3}$; $i=1,2$. $\nabla_1\nabla_2$ is the Hughes-Eckart mass polarization term. The Schrödinger equation for the system is

$$\mathcal{H}\Psi_0(r_1,r_2,r_{12}) = E_0(\mu_1,\mu_2,m_3,\sigma)\Psi_0(r_1,r_2,r_{12}), \tag{3}$$

then Eq. (3) gives the energy E_0 of the systems $(\pm m_1, \pm m_2, \mp m_3; \sigma)$, where the signs before the masses define the signs of the unitary charges.

To study the dissociation of three-particle systems, we need to know the relevant threshold for each choice of the masses. The threshold is the lowest energy of the possible two-body subsystems $(\pm m_1, \mp m_3; \sigma)$ and $(\pm m_2, \mp m_3; \sigma)$. The two-particle (reduced) Hamiltonians are

$$h^{(i)}(\mu_i,\sigma) = -\frac{1}{2\mu_i}\nabla_i^2 - \frac{e^{-\sigma r_i}}{r_i}, \quad i=1,2. \tag{4}$$

Without loss of generalization we can suppose $m_1 \geq m_2$, which implies that $\mu_1 \geq \mu_2$. We proved, using the variational principle, that for a fixed value of σ the ground-state energy of Hamiltonian $h^{(1)}$ is lower than the ground-state energy of Hamiltonian $h^{(2)}$, as follows:

$$\mathcal{E}_0^{(1)} \leq \langle h^{(1)}\rangle_2 = \mathcal{E}_0^{(2)} + \frac{1}{2}\langle\nabla^2\rangle_2\left(\frac{1}{\mu_2}-\frac{1}{\mu_1}\right) \leq \mathcal{E}_0^{(2)}, \tag{5}$$

where $\mathcal{E}_0^{(i)}$, $i=1,2$ are the ground-states energies of Hamiltonians Eq. (4) and $\langle h^{(1)}\rangle_2$ means the expectation value of this Hamiltonian in the ground-state function of $h^{(2)}$. Therefore the subsystem with the largest mass is the relevant threshold for the three-body system. We can use this information to choose an appropriate scale for the masses. For $m_1 > m_2$ and fixed screening σ the relevant threshold depends on μ_1, then we fixed the scale with the condition $\mu_1=1$, so the threshold $\mathcal{E}_0(\sigma) \equiv \mathcal{E}_0(1,\sigma)$ depends only on σ.

If the two-body system supports a bound state the relevant threshold is given by the two-body ground-state energy, else the threshold energy is equal to zero. The existence of the critical coupling for short-range one-body potentials was proven by Klaus and Simon [15] and it is defined by the condition $\mathcal{E}_0(\tilde{\sigma}_c)=0$. $\tilde{\sigma}_c$ was obtained numerically in many references [16–18]. We use a Ritz variational method as described in Ref. [16] with Laguerre polynomials up to order $n=1400$ to calculate $\mathcal{E}_0(\sigma)$ and we obtain $\tilde{\sigma}_c \approx 1.1904$. Then, a bounded two-body subsystem does not exist for $\sigma/\mu \geq \tilde{\sigma}_c$, which implies that possible three-body bound states will be Borromean states. For the calculation of the ground-state energies we used a nonorthogonal Hylleraas basis set in order to apply the Rayleigh-Ritz variational method, which is explained in Sec. III.

III. RAYLEIGH-RITZ VARIATIONAL METHOD

In order to estimate the ground-state energy, we used the Rayleigh-Ritz variational method with a nonorthogonal basis set [19]. We worked with Hylleraas basis-set functions with two fixed nonlinear parameters (γ,δ),

$$\Phi_n^{(\gamma,\delta)} = e^{-(\gamma r_1+\delta r_2)} r_1^i r_2^j r_{12}^k \quad ,n=1,\ldots,M(N), \quad i,j,k = 0,\ldots,N, \tag{6}$$

where $M(N)=(N+1)^3$ is the size of the matrices, except in the case where the two particles are identical $(m_1=m_2)$ and the basis-set functions were symmetrized. For this case the size of the matrices is $M(N)=(N+1)^2(N+2)/2$.

For a given M-function basis set $\{\Phi_i\}_1^M$, the optimal approximations to the ground-state energy and the ground-state wave function are given by the minimum eigenvalue and the corresponding eigenfunction of the equation

$$H^{(N)}\mathbf{c}^{(N)} = \lambda\mathcal{M}^{(N)}\mathbf{c}^{(N)}, \tag{7}$$

where

$$(H^{(N)})_{kj} = \langle\Phi_k|H|\Phi_j\rangle, \quad \mathcal{M}_{kj}^{(N)} = \langle\Phi_k|\Phi_j\rangle, \tag{8}$$

then

$$E_0 \leq E_0^{(N)} = \min\{\lambda_i\}, \quad \Psi_0 \simeq \Psi_0^{(N)} = \sum_{j=1}^{M(N)} c_{0,j}^{(N)}\Phi_j, \tag{9}$$

where $\{\lambda_i\}_1^M$ are the eigenvalues of $H^{(N)}$ and $\mathbf{c}_0^{(N)}$ is the eigenvector corresponding to $E_0^{(N)}$.

For an orthonormal basis set the overlap matrix $\mathcal{M}$ is equal to the identity matrix. In our case, the basis set is not orthogonal and the generalized eigenvalue problem Eq. (7) is mapped to an usual eigenvalue problem applying a Cholesky decomposition to the overlap matrix $\mathcal{M}$ [20].

The nonlinear parameters are chosen in such a way that minimizes the energy in the region of interest for $N=4$ giving $(\gamma=0.36, \delta=0.13)$. All calculations for larger values of N were done using these values for the parameters γ and δ.

In some regions of the parameter space the Hylleraas basis set could have numerical problems. In order to test our results, we also calculate the ground-state energy using a linear combination of ten exponential functions of the form $\exp(-\alpha_i r_1 - \beta_i r_2 - \gamma_i r_{12})$, $i=1,\ldots,10$. Then we use the Ritz variational method together with the pivot method for global optimization [21] to get the values of the 30 nonlinear variational parameters.

All the integrals needed for the evaluation of the matrix elements were obtained as analytic expressions [22]. In order to evaluate these integrals and the Cholesky decomposition of the overlap matrix correct up to 16 decimal places, we developed an efficient code in multiprecision FORTRAN [23], an extension of standard FORTRAN 90 that allows to work with an arbitrary number of significant figures. Once the integrals were obtained, the eigenvalue problem is solved using a standard double precision FORTRAN code.

IV. STABILITY DIAGRAM

In this section we present stability diagrams for the ground state. A stability line is defined as the line that divides a domain where a (bound) ground state exists from a domain where no three-body bound states exist.

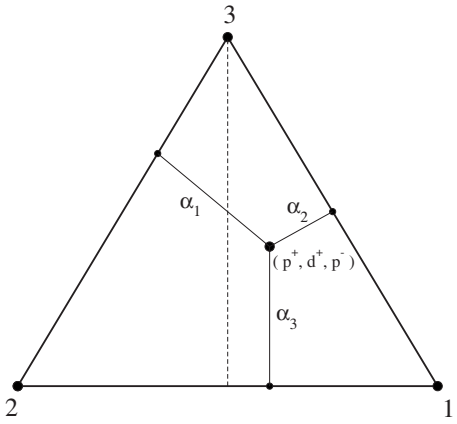

FIG. 1. Triangle of inverse masses.

As in previous works, for Coulombic interactions [3,4], the stability diagrams are presented in barycentric coordinates in the inverse masses, defined as

$$\alpha_i = \frac{1/m_i}{1/m_1 + 1/m_2 + 1/m_3}, \quad i = 1,2,3. \tag{10}$$

Note that only two of these parameters are independent since

$$\alpha_1 + \alpha_2 + \alpha_3 = 1. \tag{11}$$

Barycentric coordinates are useful for Coulombic interactions because the Coulomb potential is a homogeneous function and therefore all masses can be scaled leaving the stability diagram unchanged. This is not true for the Yukawa potential and the stability lines are in this case invariant against the simultaneous transformation $m_i \to \beta m_i$, $\sigma \to \sigma/\beta$. Taking $\beta = 1/\mu_1$ we obtain that a system with (μ_1, σ) presents the same stability diagram that the system with $(1, \mu_1\sigma)$. Then, also for Yukawa interactions, we can fix $\mu_1 = 1$ without loss of generality and we can study the stability diagrams in barycentric coordinates for different values of σ.

The stability diagram for a given value of σ is represented by an equilateral triangle, as shown in Fig. 1. Because of Eq. (11) a given value of the masses together with the condition $\mu_1 = 1$ is mapped to a point inside the triangle. Each side represents a system with one mass equal to infinity. Consequently a vertex is a system with two infinite equal masses. The symmetry axis (dashed line) in the middle of the triangle represents the case when the two particles of the same charge are identical. Then important systems such as He, H_2^+, $pp\mu^-$, $tt\mu^-$, $e^-e^-e^+$, etc. are represented by a point on this line.

Since two of the charges are equal, the stability diagram will be symmetric with respect to the symmetry axis shown in the figure. Two properties of the stability lines for Coulombian systems [3] remain true:

(i) The stability line is crossed at most one time when going from a lower vertex to the symmetry axis. The proof given in Ref. [3] does not depend of the interaction potential as it only regards the kinetic energy.

(ii) The instability domain is convex. Let us call $x_i = \frac{1}{m_i}$. Since the scale transformation in the inverse masses x space is a projection of the plane $\alpha_1 + \alpha_2 + \alpha_3 = 1$ onto the plane $x_1 + x_3 = \mu_1^{-1} = 1$, it preserves straight lines. So a proof of convexity for the $x_i's$ is also valid for the $\alpha_i's$. Suppose two points $\{x_i'\}$ and $\{x_i\}$ belong to the stability line. The threshold for the system is $\mathcal{E}_0(\sigma)$, then $E_0(x_i) = E_0(x_i') = \mathcal{E}_0(\sigma)$. According to this for any point on the line $x(\eta) = \{(1-\eta)x_i + \eta x_i'\}$ the threshold is the same. Furthermore,

$$\mathcal{H}(\eta) = \mathcal{H}((1-\eta)x_i + \eta x_i'), \tag{12}$$

$$= (1-\eta)\mathcal{H}(x_i) + \eta\mathcal{H}(x_i'), \tag{13}$$

and from the variational principle, using $\Psi_0(\eta)$ as the test function,

$$E_0(\eta) \geq (1-\eta)E_0(x_i) + \eta E_0(x_i') = \mathcal{E}_0(\sigma). \tag{14}$$

So the instability domain is always convex.

A necessary condition to enable Borromean binding can be derived as follows. Since Ψ_0 is the ground-state eigenfunction of the three-body system, from the variational theorem applied to Hamiltonian Eq. (2) with $\mu_1 = 1$, we obtain

$$E_0 = \langle \mathcal{H} \rangle_{\Psi_0} \geq \mathcal{E}_0(\sigma) + \mathcal{E}_0(\mu_2, \sigma) + \left\langle \frac{e^{-\sigma r_{12}}}{r_{12}} \right\rangle_{\Psi_0} - \frac{1}{m_3}\langle \nabla_1 \nabla_2 \rangle_{\Psi_0}, \tag{15}$$

$$E_0 - \mathcal{E}_0(\sigma) \geq \mathcal{E}_0(\mu_2, \sigma) + \left\langle \frac{e^{-\sigma r_{12}}}{r_{12}} \right\rangle_{\Psi_0} - \frac{1}{m_3}\langle \nabla_1 \nabla_2 \rangle_{\Psi_0}. \tag{16}$$

For a system to have a Borromean ground state we must have $\sigma > \tilde{\sigma}_c$, then the threshold is $\mathcal{E}_0(\sigma) = 0$ and $\mathcal{E}_0(\mu_2, \sigma) \geq \mathcal{E}_0(\sigma)$ vanishes. Then for a Borromean ground state

$$E_0 < 0 \quad \text{and} \quad E_0 \geq \left\langle \frac{e^{-\sigma r_{12}}}{r_{12}} \right\rangle_{\Psi_0} - \frac{1}{m_3}\langle \nabla_1 \nabla_2 \rangle_{\Psi_0}. \tag{17}$$

Therefore

$$\langle \nabla_1 \nabla_2 \rangle_{\Psi_0} > 0 \tag{18}$$

is a necessary condition for the existence of a Borromean state. Condition of Eq. (18) shows the importance of correlation terms in test functions in order to describe Borromean binding. Note that for uncorrelated test functions of the form $\phi_{12} = \phi(r_1)\phi(r_2)$ we have $\langle \nabla_1 \nabla_2 \rangle_{\phi_{12}} = 0$. After the calculation of the ground-state variational energy of the system, the stability line is implicitly defined by equation

$$E_0(1, \mu_2, m_3, \sigma) = E_{\text{th}}, \quad \text{where} \quad E_{\text{th}} = \begin{cases} \mathcal{E}_0(\sigma) & \text{if } \sigma < \tilde{\sigma}_c \\ 0 & \text{if } \sigma \geq \tilde{\sigma}_c. \end{cases} \tag{19}$$

From simple variational calculations a useful analytical bound can be obtained, at the expense of loosing some accuracy. For the side 2–3 ($m_1 = \infty$) there exists a critical value $(\frac{m_3}{m_2})^*(\sigma)$ at which the system becomes unstable. For this critical value there is a corresponding $\alpha_3^*(\sigma)$. Figure 2 shows the stability diagram for $\sigma = 1.1$, denoting $\alpha_3^*(1.1)$ with a blue dot. Since the variational stability line is a rigorous lower

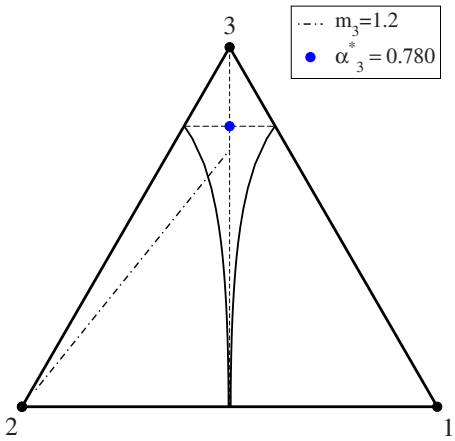

FIG. 2. (Color online) Stability diagram for $\sigma=1.1$ calculated with a basis set of size $N=14$. The dash-dotted line is the straight line corresponding to $m_3=1.2$ and μ_2 ranging from 0 to 1. The blue dot is the point $[\alpha_1=\frac{1-\alpha_3}{2}, \alpha_2=\alpha_1, \alpha_3=\alpha_3^*(1.1)=0.780]$.

bound, according to Fig. 2 all systems with $\alpha_3 > \alpha_3^*(\sigma)$ are stable for a fixed screening σ. Then from Eq. (10) it can be seen that all systems fulfilling

$$\frac{m_3}{m_1}\left(\frac{m_1}{m_2}+1\right) < \left(\frac{1}{\alpha_3^*(\sigma)}-1\right) \tag{20}$$

are stable. This result is applicable to any value of σ down to $\sigma=0$, although it is more accurate for $\sigma \gtrsim \tilde{\sigma}_c$. In Fig. 3 we show the function $\sigma(\alpha_3^*)$. For the critical screening we get $\alpha_3^*(\tilde{\sigma}_c)=0.880$, then all systems fulfilling

$$\frac{m_3}{m_1}\left(\frac{m_1}{m_2}+1\right) < 0.136 \tag{21}$$

have a Borromean ground state at the critical screening.

In Fig. 2 it can be seen that the symmetry axis is stable for $\sigma=1.1$. If the screening is increased, the stable domain is reduced until the region of stability is the upper vertex (a

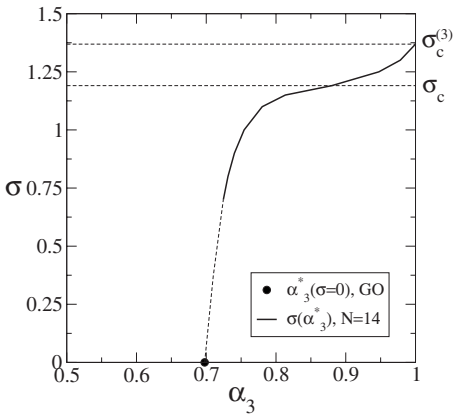

FIG. 3. The function $\sigma(\alpha_3)$ for which systems $(m_1=\infty, m_2, m_3=1)$ become unstable, obtained from variational calculations. Also, the point $\alpha_3^*(\sigma=0)$, obtained with global optimization for the Coulomb limit and the point $\sigma_c^{(3)}$ where all three-body systems are unstable.

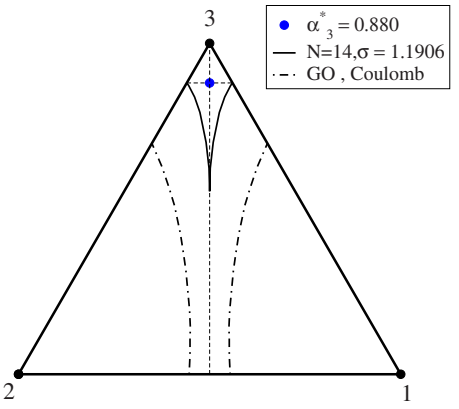

FIG. 4. (Color online) Stability diagram for $\sigma=1.1906 \approx \tilde{\sigma}_c$ calculated with a base of size $N=14$ (for symmetrical systems results are up to $N=17$). The blue dot is the point $[\alpha_1=\frac{1-\alpha_3}{2}, \alpha_2=\alpha_1, \alpha_3 \equiv \alpha_3^*(1.1906)=0.880]$. The stability line for the Coulomb limit $\sigma=0$ calculated with a global optimization algorithm [21] is also shown.

symmetric molecule with two infinitely heavy nuclei and one light particle). Figure 4 shows the reduction of the stability domain for the critical screening. In Fig. 5 we plot the stability line $\sigma(\alpha_3)$ for which symmetrical systems become unstable. It can be seen that all systems, symmetrical or not, are unstable for $\sigma > \sigma_c^{(3)}=1.369$. A previous estimation for this value $\sigma_c^{(H_2^+)}=1.373(4)$, obtained for H_2^+ using a nonadiabatic quantum Monte Carlo study, was reported in Ref. [6]. This result agrees with our calculations within statistical error.

In Sec. VI we use the finite-size scaling method (FSS) to obtain the critical behavior of these systems. It is shown that a more accurate value for the stability line can be obtained using the scaling properties of the truncated basis set. The stability line obtained with FSS is also shown in Fig. 5. This line indicates that all symmetrical systems with three equal masses, such as Ps^-, are Borromean at $\sigma=\tilde{\sigma}_c$. Then, FSS gives us a strong numerical evidence for the existence of Borromean systems.

It is known [5,24] that for Coulomb interactions $(\sigma=0)$ all systems that lie in the symmetry axis are stable. But, as we can see in Figs. 4 and 5, at the critical screening this is no

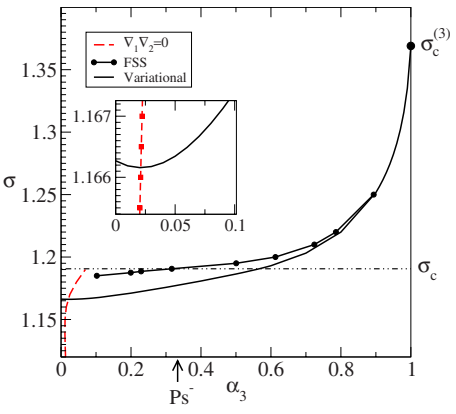

FIG. 5. (Color online) Stability line $\sigma(\alpha_3)$ for symmetrical systems. Inset shows a very narrow domain near $\alpha_3=0$, where an instability gap appears on the symmetry axis.

longer true. Then, there is a value of the screening parameter $0<\sigma^*<\tilde{\sigma}_c$ below which the symmetry axis becomes stable. The variational estimation for this value is $\sigma^*\simeq 1.1661$. Increasing σ, an instability gap appears on the symmetry axis, i.e., a very small fraction of systems near $\alpha_3=0$ are stable while the systems around $\alpha_3\sim 0.02$ are not. The systems from the upper vertex down to $\alpha_3\sim 0.02$ are stable; although for the Coulomb interaction it was suggested [5] that when the charge of the particles is varied the stability region splits into two islands; for our model a very small increase in σ makes the lower domain disappear. Since this could be a numerical misleading, a deeper analysis on whether this domain exists or not should be made. As an starting point we can address that, as can be seen in Fig. 5, the mass polarization term vanishes at this value, consequently the stability line derivative vanishes at the point where the gap appears. This was also observed for Coulomb interaction [25], but the variable was the relative charge of the particles.

V. EFIMOV EFFECT FOR THREE-UNIT CHARGES

The Efimov effect is present in many three-body systems, although the most widespread version is the one with three identical bosons [11,12,26–29]. Recently, the first experimental Efimov state on cold cesium atoms was reported [30]. This result has motivated new research on the subject. In particular, Lee *et al.* [31] claimed that the observed state is not an Efimov state but a Borromean molecular state.

The effect consists in the appearance of a universal set of three-body bound states at a point where the two-body scattering length a diverges. The divergence of the scattering length occurs when a two-body bound state enters the continuum threshold by tuning some Hamiltonian parameter. Then, the divergence of a is actually a near-threshold phenomenon that, in our case, corresponds to setting the screening to the critical value $\tilde{\sigma}_c$. The set of three-body states fulfills the well-known geometric relationship [11,26]

$$\frac{E_{n+1}}{E_n}=e^{-2\pi/s_0}, \tag{22}$$

with $s_0=1.006\,24$.

Near the divergence of a these states are expected to hit the continuum threshold. The continuum threshold for $a>0$ is the two-body bound-state energy, while for $a<0$ it corresponds to three unbound particles. The universal asymptotic function for the number of bound states, first obtained by Efimov [11], is

$$N\to\frac{s_0}{\pi}\ln\frac{|a|}{l}, \tag{23}$$

where l is a natural length scale, related to the range of the interactions. The natural length scale is chosen of order $\frac{1}{\sigma}$. This formula shows that other possibility to obtain infinite bound states is in the scaling limit $l\to 0$, although we will focus on the divergence of a.

For systems of two identical fermions interacting with a different particle, some results were obtained [26,27]. One of the differences between this system and the one with bosons is that the universal constant $e^{-\pi/s_0}$ becomes a function of $\frac{m_1}{m_3}$. Moreover, the effect disappears for $\frac{m_1}{m_3}<13.6$ because the scaling constant e^{π/s_0} diverges. When $\frac{m_1}{m_3}\to\infty$ the scaling constant approaches 1. All these previous works do not take into account repulsive interactions between particles, as we do, but the universal behavior should not be affected by the repulsion term.

In this work we obtain numerical evidence of this effect, Fig. 6 shows the energy curves in scaled variables for $m_1/m_3=10$, 198, and $m_p/m_e=1836.15$. The scaling constants obtained for these states are $e^{\pi/s_0}\approx\infty$, 1.76, and 1.45 and for $m_1/m_3=100$ we obtained $e^{\pi/s_0}\approx 2.0$. Moreover, the effect appears only if the particles 1 and 2 are identical. For distinguishable particles there are three different scattering lengths $(a_{ij},\ i,j=1,2,3)$, corresponding to the three possible two-body subsystems. As discussed in Ref. [26], the Efimov effect does not appear if only one scattering length diverges. In general, more than one scattering length should diverge in order to see the effect. The scattering for the two-body subsystem a_{12} is irrelevant, since they are repulsive particles interacting through a short-range potential. Therefore, there are two relevant scattering lengths a_{13} and a_{23}, which diverge when the two-body screenings $\tilde{\sigma}_i=\sigma/\mu_i$, $i=1,2$ are equal to the critical value $\tilde{\sigma}_c$. The condition $\mu_1=1$ gives $\tilde{\sigma}_1=\sigma$, so a_{13} diverges only for $\sigma=\tilde{\sigma}_c$. In order to make both scattering lengths diverge, μ_2 must also be unity. We show in Fig. 7 the number of bound states against σ for H_2^+, $m_1=m_2=m_p$, and $m_3=m_e$. This result supports the assumption that this molecule presents Efimov effect when the screening is critical.

VI. NEAR-THRESHOLD BEHAVIOR

Another interesting issue is the asymptotic behavior of the ground-state energy near the critical line. We can define a critical exponent α for the energy [32] as follows:

$$E_0(\lambda)-E_{\text{th}}\sim -e(|\lambda_c-\lambda|)^{\alpha},\quad \lambda\uparrow\lambda_c^- \tag{24}$$

where λ represents one of the parameters of the Hamiltonian (μ_2, m_3 or σ), E_{th} is the threshold energy, and $\uparrow$ means that the limit is taken inside the bound-state region.

The existence of a bound state at the critical point is related to the critical exponent α. For a large class of Hamiltonians, Simon [33] showed that the critical exponent α is equal to 1 if and only if the Hamiltonian has a normalizable eigenfunction at the threshold. If the Hamiltonian does not support a bound state at the threshold, then $\alpha>1$. The existence of a normalizable (localized) state at the critical point characterizes the near-threshold scattering properties.

In order to calculate the critical exponent, we use FSS [32] to obtain the critical screening σ_c and the critical exponent α. This method has been successfully applied to calculate the exponent for the energy of several one-, two-, and three-particle systems (see [32] and references therein), in the calculation of critical exponents for the near-threshold entanglement of two-electron systems [34,35], and for the study of the stability of hydrogen-antihydrogen-like quasimolecules [36]. In the FSS approach, the ansatz is to assume that there is a scaling function such that

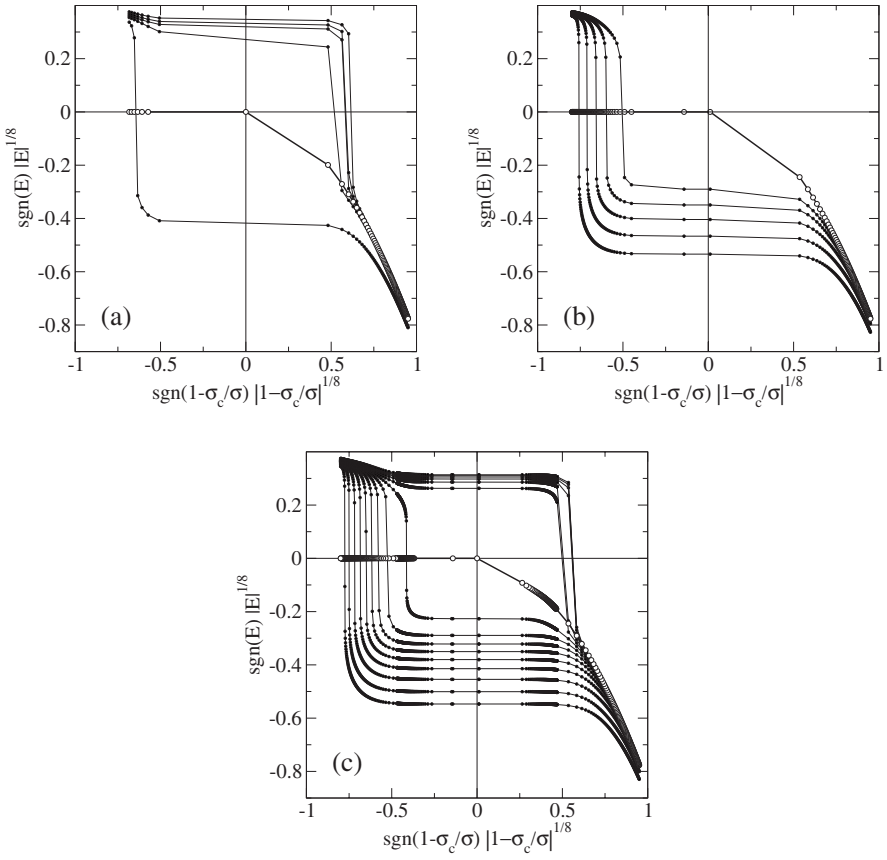

FIG. 6. The lower eigenvalues obtained from a Rayleigh-Ritz variational method with $N=17$ for symmetric system for (a) $m_1/m_3=10$, (b) $m_1/m_3=198$, and (c) $m_1/m_3=m_p/m_e=1836.15$ as a function of the scaled screening σ. Clearly there are no Efimov trimers for $m_1/m_3=10$ [27].

$$\langle \mathcal{O} \rangle_{\lambda}^{(N)} \approx \langle \mathcal{O} \rangle_{\lambda} F_{\mathcal{O}}(N|\lambda - \lambda_c|^{\nu}), \tag{25}$$

where $\langle \mathcal{O} \rangle_{\lambda}^{(N)}$ is the order N expectation value of the operator $\mathcal{O}$ evaluated in the truncated basis set. It is further assumed that the scaling exponent ν is unique for all the operators and a different scaling function $F_{\mathcal{O}}$ exists for each operator. We want to study the critical exponent of the energy, then $\mathcal{O}$ will be the Hamiltonian. As explained in Ref. [32], we calculate the energy and the expectation value $\langle \frac{\partial \mathcal{H}}{\partial \lambda} \rangle$ for two different basis-set sizes N and N'. Then, the function

$$\Gamma_{\alpha}(\lambda;N,N') = \frac{\ln(E_{\lambda}^{(N)}/E_{\lambda}^{(N')})}{\ln(E_{\lambda}^{(N)}/E_{\lambda}^{(N')}) - \ln(\langle \frac{\partial \mathcal{H}}{\partial \lambda} \rangle^{(N)} / \langle \frac{\partial \mathcal{H}}{\partial \lambda} \rangle^{(N')})} \tag{26}$$

is independent of N and N' at $\lambda=\lambda_c$ and gives the value of the critical exponent α,

$$\Gamma_{\alpha}(\lambda_c;N,N') = \alpha. \tag{27}$$

For the case of two identical particles, $\mu_2=1$, the parameter λ is chosen equal to $\frac{1}{m_3}$. As it is shown in Eq. (2), this is the coupling of the Hughes-Eckart term. The asymptotic behavior of the energy, for fixed σ, is then

$$E_0(m_3^{-1},\sigma) - \mathcal{E}_0(\sigma) \sim -e\{m_3^{-1} - [m_3^{(c)}(\sigma)]^{-1}\}^{\alpha(\sigma)}. \tag{28}$$

In this equation we take into account the possible dependence of the critical exponent with the screening. This dependence is expected mostly because the threshold two-body energy also has a critical point at $\sigma=\tilde{\sigma}_c$, $\mathcal{E}_0(\sigma) \sim -e(\sigma - \tilde{\sigma}_c)^2$. For values $\sigma < \tilde{\sigma}_c$ the threshold is negative and there is a normalizable wave function for the two-body system. For screening values $\sigma > \tilde{\sigma}_c$ the threshold energy is zero, so a change in the critical behavior of the three-body system could be detected in the exponent α as a function of the screening σ. This dependence of the critical exponent α as

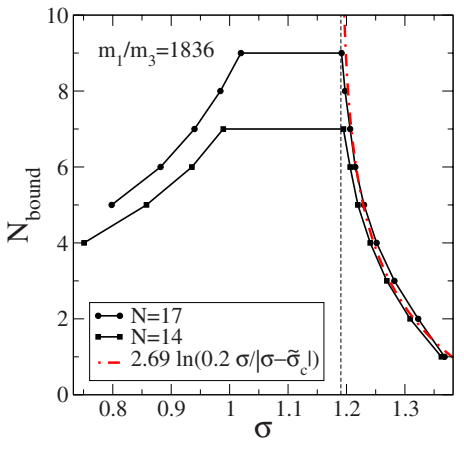

FIG. 7. (Color online) Number of bound states as a function of σ for two different basis-set sizes, $N=14$ and 17, for H_2^+ ($m_1=m_2=m_p, m_3=m_e$). The number of bound states is maximum near $\tilde{\sigma}_c$. The dash-dotted red line is the universal function number of bound states Eq. (23) calculated using the values $s_0/\pi \approx 2.69$ and $\tilde{\sigma}_c = 1.1904$.

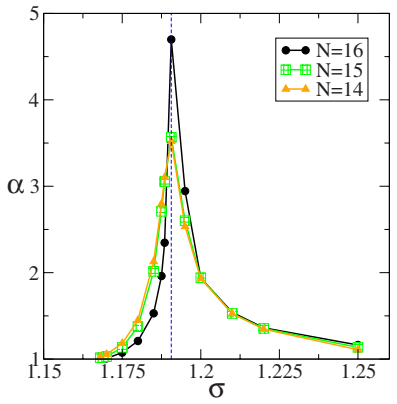

FIG. 8. (Color online) The critical exponent of the energy α against the screening σ for symmetrical systems obtained from the FSS method with $N=14$, 15, and 16. The blue dashed line represents the two-body critical line $\sigma=\tilde{\sigma}_c$, which separates usual from Borromean states.

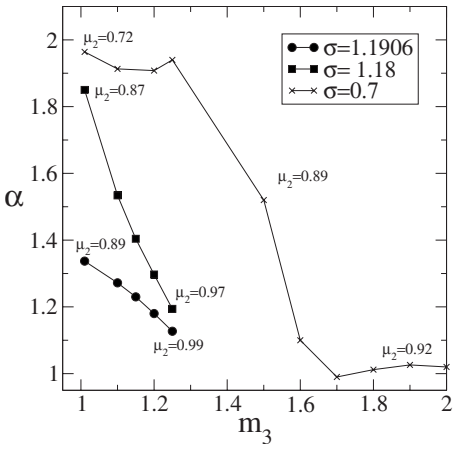

FIG. 9. The critical exponent of the energy α as a function of the mass m_3 for asymmetrical systems for different screening values obtained with FSS method. Results for base size up to $N=14$ are shown. The values of μ_2 for the stability line are shown for some points.

a function of σ, is shown in Fig. 8. The peak at $\sigma=\tilde{\sigma}_c$ could be due to the change from usual to Borromean behavior of the near-threshold ground state.

When $\mu_2 \neq 1$, particles 1 and 2 are distinguishable and the parameter used in Eq. (26) was $\lambda=\mu_2^{-1}$, the screening and the mass m_3 were kept fixed. Figure 9 shows the energy exponent α as a function of the mass m_3 for different choices of the screening σ. The values of μ_2 for the stability line are shown for some points. It can be seen that the exponent changes from 2 to 1 when going from fully asymmetric configurations to nearly symmetric configurations $\mu_2 \simeq 1$. This behavior is likely to happen because the value $\alpha=1$ is expected for $\mu_2=\mu_1$ [13], otherwise $\alpha>1$.

VII. CONCLUSIONS

The stability diagram for three-unit charges in a Debye plasma was investigated. The stability domain for the ground-state energy was obtained for several values of the screening parameter. We showed that the stability diagram for the screened-Coulomb three-body Hamiltonian presents regions with "usual" bound states and regions with Borromean bound states. We presented rigorous variational bounds for the region of Borromean binding. Our calculations also give numerical evidence for the possible existence of Efimov states.

Among other systems, we proved that $pp\mu^-$, $pd\mu^-$, $pt\mu^-$, and $dt\mu^-$ (and changing $\mu^- \to e^-$) present Borromean binding when the particles interact through a Yukawa potential. There is also strong evidence, obtained using the FSS method, that the Ps^- has a Borromean ground state. According to this, all three-body systems with two identical particles $(\pm m_1, \pm m_1, \mp m_3)$ and $m_3/m_1 \leq 1$ have a Borromean ground state at $\sigma=\tilde{\sigma}_c$.

Numerical evidence of the existence of Efimov states was given. The simultaneous divergence of the scattering lengths a_{13} and a_{23} gives rise to the effect for symmetrical systems at the critical two-body coupling $\tilde{\sigma}_c \approx 1.1904$. The effect is detected for $\frac{m_1}{m_3} \gtrsim 100$ and is lost for $\frac{m_1}{m_3} \lesssim 10$. A result on this matter was reported [27] for identical fermions on general grounds with no repulsive interaction. Here we find a good agreement with this reference including the repulsive interaction. This agreement supports the theory which states that the interaction between identical particles in a H_2^+-like system is irrelevant as long as it is of shorter range than $1/r^2$. The reason of this is that the two-body bound-state density is delocalized, then the short-range interaction between identical particles vanishes [12,13]. In particular we showed that not even the sign of the interaction is relevant for the appearance of the effect.

The critical exponent of the system was also calculated. The numerical results are not conclusive, but they show the main aspects of the near-threshold phenomena. A change of critical behavior from the Borromean to the non-Borromean region was observed in the critical exponent α of the energy. Discrepancies between the different approaches to the critical point show that more analyses and new methods are needed to clarify this matter. Another change in the critical behavior was found when the symmetry between identical particles $(m_1=m_2)$ is broken $(m_1 \neq m_2)$ in the non-Borromean domain. The symmetric systems have a critical exponent $\alpha=1$, as it is discussed in Ref. [13]. Asymmetrical systems have a critical exponent $\alpha>1$ according to the present results. More evidence is needed on this subject, but we suggest that the reason for symmetrical systems to have an exponent $\alpha=1$ is the fermionic symmetrization, which is broken when the particles are not identical.

ACKNOWLEDGMENTS

We would like to thank Belén Franzoni and Alejandro Ferrón for useful discussions and critical reading of the paper. We would like to acknowledge SECYT-UNC, CONICET, and FONCyT for partial financial support of this project.

[1] H. Bethe, Z. Phys. **57**, 815 (1929).
[2] E. A. Hylleraas, Z. Phys. **63**, 297 (1930).
[3] A. Martin, J.-M. Richard, and T. T. Wu, Phys. Rev. A **46**, 3697 (1992).
[4] E. A. Armour and W. B. Brown, Acc. Chem. Res. **26**, 168 (1993).
[5] E. A. G. Armour, J. M. Richard, and K. Varga, Phys. Rep. **413**, 1 (2005).
[6] L. Bertini, M. Mella, D. Bressanini, and G. Morosi, Phys. Rev. A **69**, 042504 (2004).
[7] Sabyasachi Kar and Y. K. Ho, Phys. Rev. A **75**, 062509 (2007).
[8] Sabyasachi Kar and Y. K. Ho, Phys. Rev. A **71**, 052503 (2005).
[9] Sabyasachi Kar and Y. K. Ho, Phys. Rev. E **70**, 066411 (2004).
[10] A. S. Jensen, K. Riisager, and D. V. Fedorov, Rev. Mod. Phys. **76**, 215 (2004).
[11] V. Efimov, Phys. Lett. **33B**, 563 (1970).
[12] A. C. Fonseca, E. F. Redish, and P. E. Shanley, Nucl. Phys. A. **320**, 273 (1979).
[13] F. M. Pont and P. Serra, J. Phys. A **41**, 275303 (2008).
[14] R. Guardiola and J. Navarro, Phys. Rev. Lett. **84**, 1144 (2000).
[15] M. Klaus and B. Simon, Ann. Phys. (N.Y.) **130**, 251 (1980).
[16] P. Serra, J. P. Neirotti, and S. Kais, Phys. Rev. A **57**, R1481 (1998).
[17] F. J. Rogers, H. C. Graboske, and D. J. Harwood, Phys. Rev. A **1**, 1577 (1970).
[18] O. A. Gomes, H. Chacham, and J. R. Mohallem, Phys. Rev. A **50**, 228 (1994).
[19] E. Merzbacher, *Quantum Mechanics*, 3rd ed. (Wiley, New York, 1998).
[20] W. H. Press, S. A. Teukolsky, W. T. Vetterling, and B. P. Flannery, *Numerical Recipes in Fortran 77*, 2nd ed. (Cambridge University Press, Cambridge, 1996).
[21] P. Serra and A. F. Stanton, S. Kais, and R. E. Bleil, J. Chem. Phys. **106**, 7170 (1997).
[22] R. A. Bonham and D. A. Kohl, J. Chem. Phys. **45**, 2471 (1966).
[23] D. H. Bailey, ACM Trans. Math. Softw. **21**, 379 (1995).
[24] R. N. Hill, J. Math. Phys. **18**, 2316 (1977).
[25] S. Kais and Q. Shi, Phys. Rev. A **62**, 060502(R) (2000).
[26] E. Braaten and H.-W. Hammer, Phys. Rep. **428**, 259 (2006).
[27] D. S. Petrov, Phys. Rev. A **67**, 010703(R) (2003).
[28] A. Bulgac and V. Efimov, Sov. J. Nucl. Phys. **22**, 153 (1976).
[29] A. E. A. Amorim, T. Frederico, and L. Tomio, Phys. Rev. C **56**, R2378 (1997).
[30] T. Kraemer, M. Mark, P. Waldburger, J. G. Danzl, C. Chin, B. Engeser, A. D. Lange, K. Pilch, A. Jaakkola, H.-C. Nägerl, and R. Grimm, Nature (London) **440**, 315 (2006).
[31] M. D. Lee, T. Kohler, and P. S. Julienne, Phys. Rev. A **76**, 012720 (2007).
[32] S. Kais and P. Serra, Adv. Chem. Phys. **125**, 1 (2003).
[33] B. Simon, J. Funct. Anal. **25**, 338 (1977).
[34] O. Osenda and P. Serra, Phys. Rev. A **75**, 042331 (2007).
[35] O. Osenda and P. Serra, J. Phys. B **41**, 065502 (2008).
[36] A. Ferrón, P. Serra, and S. Kais, Phys. Rev. A **77**, 052505 (2008).